Accelerated Accumulation of Amyloid β Proteins on Oxidatively Damaged Lipid Membranes†

Vishwanath Koppaka‡ and Paul H. Axelsen*,‡,§

Departments of Pharmacology, and Medicine, Infectious Disease Section, The Johnson Foundation for Molecular Biophysics, University of Pennsylvania School of Medicine Philadelphia, Pennsylvania 19104-6084

Received March 17, 2000; Revised Manuscript Received May 23, 2000

ABSTRACT: The fully developed lesion of Alzheimer's Disease is a dense plaque composed of fibrillar amyloid β-proteins with a characteristic and well-ordered β-sheet secondary structure. Because the incipient lesion most likely develops when these proteins are first induced to form β-sheet secondary structure, it is important to understand factors that induce amyloid β-proteins to adopt this conformation. In this investigation we used a novel form of infrared spectroscopy that can characterize the conformation, orientation, and rate of accumulation of the protein on various lipid membranes to determine whether oxidatively damaged phospholipid membranes induce the formation of β-sheet secondary structure in a 42-residue amyloid β-protein. We found that membranes containing oxidatively damaged phospholipids accumulated amyloid β-protein significantly faster than membranes containing only unoxidized or saturated phospholipids. Accelerated accumulation was also seen when 3 mol % G_{M1} ganglioside was incorporated into a saturated phosphatidylcholine membrane. The accumulated protein more completely adopted a β-sheet conformation on oxidized membranes, and the plane of the β-sheet was oriented parallel to the plane of the membrane. These results indicate that oxidatively damaged phospholipid membranes promote β-sheet formation by amyloid β-proteins, and they suggest a possible role for lipid peroxidation in the pathogenesis of Alzheimer's Disease.

Amyloid β-proteins (Aβ-proteins) are 39−42 residue polypeptides that accumulate as dense plaques in the brain parenchyma and cerebrovascular tissues of patients with Alzheimer's disease. They are derived from a membrane-spanning glycoprotein known as β-amyloid precursor protein (βAPP) (*1*) by the proteolytic action of γ-secretases (*2*−*5*). Although Aβ-proteins and various portions of these proteins have direct neurotoxic effects (*5*−*10*), it remains unclear whether amyloid plaques are mediators or byproducts of the pathogenic process that leads to Alzheimer's disease.

The 40-residue form of Aβ-(Aβ40) along with its various amino- and carboxy-terminal derivatives appear to be the predominant forms of Aβ-in cortical brain (*11*), cerebrovascular amyloid deposits (*12*), and at least some forms of hereditary amyloidosis (*13*). The 42-residue form (Aβ42), on the other hand, appears to associate with G_{M1} ganglioside and predominate in early diffuse plaques (*12*, *14*−*16*). Both proteins are produced intracellularly, but in different cellular organelles (*4*, *17*) and by the action of different enzymes (*2*, *3*, *5*, *18*). Due to its prevalence in earlier lesions, its lower solubility, and its tendency to form and stimulate the formation of fibrillar aggregates, it has been proposed that Aβ42 serves to nucleate amyloid plaque formation (*19*−*22*).

Numerous investigations of Aβ40 and Aβ42 have been conducted into their physical properties in an attempt to understand their role in the pathogenesis of Alzheimer's Disease. Although a multitude of factors have been shown to stimulate folding, refolding, and even unfolding of these proteins under various circumstances (*23*−*32*), the fundamental reason amyloid plaques form in patients with Alzheimer's Disease remains elusive.

Several lines of reasoning converge to suggest that oxidatively damaged phospholipids may stimulate the formation of amyloid plaques by Aβ42. The central observation is that phospholipids and gangliosides exert a profound influence on the secondary structure of Aβ-proteins, in many cases inducing β-structure (*15*, *24*, *26*, *28*−*31*). Along with this observation, we know that lipids in the human brain contain a variety of unsaturated fatty acyl chains in relatively high concentration (*33*), that olefinic groups in these lipids are highly susceptible to reactions with reactive oxygen species, and that as a consequence, oxidative changes due to free radicals and other reactive oxygen species are probably the chief mediators of age-related changes in brain lipid (*34*−*36*). Finally, it has been recognized that brain tissues tend to have low levels of naturally occurring antioxidants (*37*), that patients with Alzheimer's Disease tend to have much lower plasma levels of vitamin E (*38*, *39*), and that vitamin E has a salutary effect on the clinical course of Alzheimer's Disease (*40*).

These observations suggest that oxidative damage may have significant consequences on the interaction of Aβ42 with phospholipid membranes. Therefore, we have investi-

† Supported by NIH GM54617 and a grant-in-aid to PHA from the American Heart Association.

* To whom correspondence should be addressed. Phone: (215) 898-9238. Fax: (215) 573-2236. E-mail: axe@pharm.med.upenn.edu.

‡ Department of Pharmacology.

§ The Johnson Foundation for Molecular Biophysics.

10.1021/bi000619d CCC: $19.00 © 2000 American Chemical Society
Published on Web 07/21/2000

gated the effects of oxidative damage on the interaction of Aβ42 with phospholipid membranes using a novel form of polarized attenuated total internal reflection Fourier transform infrared (PATIR−FTIR) spectroscopy that yields quantitative information about the rate of accumulation, the conformation, and the orientation of proteins as they interact with a fully hydrated lipid monolayer in a Langmuir trough (*41*−*46*). Our results indicate that the formation of β-structure by Aβ42 is accelerated by oxidatively damaged membranes. The β-structure is antiparallel and oriented parallel to the plane of the membrane. These and other observations made in the course of this investigation suggest a possible mechanism whereby oxidatively damaged membranes specifically induce the formation of antiparallel β-structure by amyloid β-proteins.

EXPERIMENTAL PROCEDURES

Materials. Lyophilized Aβ42 was purchased from Bachem Bioscience Inc. (King of Prussia, PA) and used without further purification. This material used in these experiments was shown to electrophorese as a single band, and to have the expected molecular weight (4514) by MALDI-TOF mass spectrometry. Some lots of material we received did not pass these tests. Synthetic dimyristoylphosphatidylcholine (DMPC) and 1-stearoyl-2-arachidonyl-*sn*-glycero-3-phosphocholine (SAPC) were purchased from Avanti Polar Lipids (Alabaster, AL). The latter was stored in chloroform and under Argon in sealed glass ampules at −20 °C until the day of use. Correct molecular weight and the absence of major impurities in the lot of SAPC used for this work was confirmed by electrospray ionization mass spectrometry. DMPC and unoxidized SAPC were prepared for use by evaporating the chloroform under nitrogen and redissolving in 9:1 hexane: ethanol. Ganglioside G_{M1} (purity > 98%) was purchased from Calbiochem (La Jolla, CA). Butylated hydroxytoluene (BHT) was purchased from Sigma. The protein was dissolved in hexafluoro-2-propanol (HFIP) and stored at −20 °C. Before each experiment, an aliquot of this stock solution was evaporated and redissolved at a concentration of 90 μM protein in 30 mM HEPES in D_2O, pD 7.5. Lipid concentrations were determined by phosphate analysis (*47*).

Preparation of Oxidized Phospholipid. Stock solutions of SAPC in chloroform were dried under nitrogen, suspended in nitrogen-saturated 50 mM Tris, pH 7.5, at a concentration of approximately 1 mM, and extruded through a 0.1 μm polycarbonate filter to produce unilammelar vesicles. This vesicle suspension was then adjusted to a concentration of approximately 100 μM with the same buffer and oxidized at room temperature with 200 μM $CuSO_4$ and 2 mM H_2O_2. The rate of conjugated diene formation was monitored by UV spectroscopy at 234 nm (*48*). By this measure, oxidation proceeded at a rate that is 10-fold that which occurred without $CuSO_4$ and H_2O_2. After 105 min of oxidation, the reaction mixture was extracted twice with a chloroform: methanol mixture (2:1 v/v). The organic phase was removed, evaporated under nitrogen, and dissolved in 9:1 hexane: ethanol. This extract was examined with ESI-MS, revealing peaks at *m*/*z* 810 and 832 (corresponding to protonated and sodiated forms of SAPC), and additional peaks corresponding to the addition of one to four O_2 molecules.

Lipid monolayers were prepared in a Langmuir trough by applying lipids dissolved in hexane:ethanol to the surface

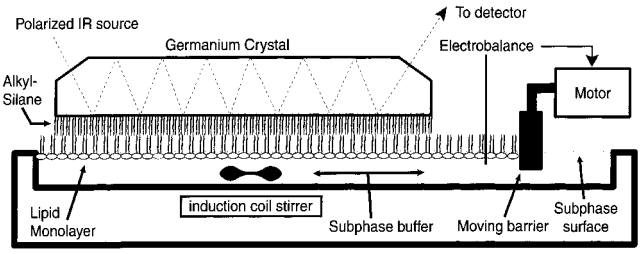

FIGURE 1: Instrument schematic. Not to scale: beam internally reflects off the bottom surface 21 times in a 2 × 10 × 52 mm crystal. Membrane surface pressure is set and maintained by a feedback loop involving an electrobalance Wilhelmy plate for pressure measurement and a moving barrier. Spectra are recorded before and after introduction of protein sample into the 6 mL subphase volume.

of a buffer containing 30 mM HEPES in D_2O at pD 7.5. The lipids applied in this manner consisted of either 100% DMPC or mixtures of 3 mol % G_{M1} and 97 mol % DMPC; 20 mol % SAPC (unoxidized), 80 mol % DMPC, and 1 mol % BHT; or 20 mol % SAPC (oxidized) and 80 mol % DMPC. The monolayer formed in the trough at the air−water interface was compressed to a surface pressure of 20 dynes/cm and applied onto a silane-treated germanium crystal as illustrated (Figure 1) and previously described (*42*, *46*). The protein was introduced in 8 μg aliquots to a continuously stirred subphase compartment containing 6 mL of subphase buffer.

Polarized attenuated total internal reflection Fourier transform infrared (PATIR−FTIR) spectra were collected in rapid-scanning mode as 1024 co-added interferograms using a Bio-Rad FTS-60A spectrometer, a liquid-nitrogen cooled MCT detector, an aluminum wire grid polarizer, a resolution of 2 cm^{-1}, scanning speed of 20 MHz, triangular apodization, and one level of zero filling. As is typical for our instrument, no baseline correction, water vapor subtraction, or smoothing manipulations were necessary. An enclosure around the Langmuir trough is filled with argon to avoid spontaneous air oxidation of lipids at the air−water interface. For the collection of spectra in kinetics mode, the polarizer was removed (to improve signal intensity), the resolution was set to 4 cm^{-1}, the scanning speed was increased to 40 kHz, and a complete spectrum was recorded every 15 s by coadding 78 interferrograms. All spectroscopic studies were performed at 27 °C, i.e., slightly above the phase transition temperature of DMPC.

Dichroic ratios, $R_z = \int A_{\parallel} / \int A_{\perp}$, were derived from the polarized absorption spectra using integrated areas of characteristic absorption bands, $\int A$, as determined by linked analysis (*46*). Dichroic ratios were converted to order parameters, $S(R_z)$, according to

$$S(R_z) = \frac{\langle E_x^2 \rangle - R_z \langle E_y^2 \rangle + \langle E_z^2 \rangle}{\langle E_x^2 \rangle - R_z \langle E_y^2 \rangle - 2\langle E_z^2 \rangle}$$

where angle brackets indicate mean values, and the two-phase approximation is used to calculate the mean electric field amplitude components $\langle E_x \rangle$, $\langle E_y \rangle$, and $\langle E_z \rangle$ where x is the direction of beam propagation, y is oriented transverse to the beam propagation in the plane of the membrane, and z is normal to the membrane (*43*, *44*). An order parameter of 1.0 indicates a uniform orientation perpendicular to the

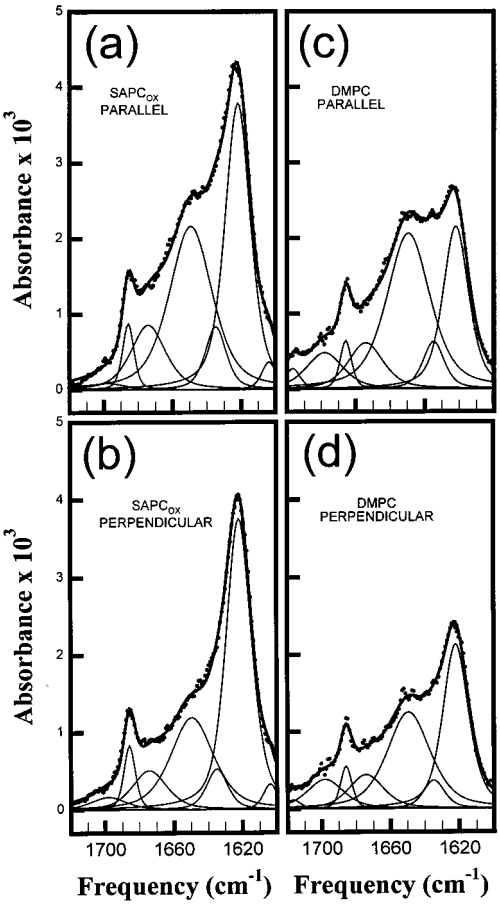

FIGURE 2: Amide I bands in the PATIR−FTIR spectra of Aβ42 bound to a monolayer composed of 20 mol % oxidized SAPC and 80 mol % DMPC (a and b) and 100% DMPC (c and d). Parallel-polarized spectra are shown in panels a and c; perpendicularly polarized spectra in panels b and d. Experimental data represented by discrete symbols; individual component bands obtained from Irfit are shown in thin lines, and the sum of the fit components is represented by a thick solid line overlying most of the data points.

membrane surface, while a value of −0.5 indicates a uniform orientation parallel to the membrane. An order parameter of 0.0 may indicate either a uniform orientation at the magic angle (54.7° relative to the surface normal), complete disorder as in an isotropic system, or any other orientation distribution for which γ is the "tilt" angle between the molecular axis and the surface normal and $\langle \cos^2 \gamma \rangle = {}^1/_3$. The tilt angles for β-sheets were determined according to Marsh (*49*).

RESULTS

Conformation and Orientation of Aβ42. The PATIR−FTIR spectra of Aβ42 on oxidized and unoxidized membranes after 60 min of accumulation are compared in Figure 2. The overall spectral amplitude from the oxidized membrane (Figure 2, panels a and b) is twice as large as that seen in the unoxidized membrane (Figure 2, panels c and d). In both membranes, the prominent feature at ∼1623 cm^{-1} and the smaller feature at ∼1685 cm^{-1} constitute the characteristically split spectral signature of antiparallel β-sheet conformation (*50*). Because this split absorption signal arises from complex interactions between polypeptide strands, it is unlikely to originate from the binding of single Aβ42 molecules to lipid in an extended conformation, and it most likely represents intermolecular or intramolecular formation of antiparallel β-sheets by Aβ42. The broader and less conspicuous component at ∼1650 cm^{-1} suggests that some helical or random secondary structure is also present. The characteristic spectral features of an antiparallel β-sheet are much more prominent than the broad helical/random component at ∼1650 cm^{-1} in the oxidized membrane compared to the unoxidized membrane.

Table 1: Dichroic Ratios and Order Parameters[a] for the Amide Bands Corresponding to Aβ42 Adsorbed to Phospholipid Monolayers

monolayer composition	amide I bands	∼1623 cm^{-1}	∼1645 cm^{-1}	∼1685 cm^{-1}
SAPC (oxidized)/ DMPC (20:80)	R_z	1.0	1.85	1.27
	$S(R_z)$	−0.42	−0.12	−0.31
DMPC	R_z	0.96	1.72	1.19
	$S(R_z)$	−0.44	−0.16	−0.34

[a] Order parameters were calculated using the "two-phase" approximation (*43*, *44*). The isotropic dichroic ratio [R_{ISO}, the ratio for which $S(R_z) = 0$] for this instrument is 2.33.

The infrared extinction coefficient for β-structure is probably higher than for helical or random coil protein (*51*); therefore, all subsequent analyses are performed on the integrated absorbance of the band at ∼1624 cm^{-1} that is most characteristic of β-structure. Because the subphase protein concentration was identical in every experiment, and both spectra were recorded at the same interval after protein injection, the spectra suggest that oxidatively damaged membranes have an increased avidity for Aβ42 in a β-sheet conformation. See control experiments, below.

The ratio of the amplitudes of the 1623 and 1685 cm^{-1} bands in Figure 2 for both oxidized and unoxidized membranes are similar suggesting that the protein has some antiparallel β-sheet structure on both membranes. The dichroic ratios and order parameters obtained for the binding of Aβ42 to membranes are given in Table 1. The dichroic ratio of ∼1.0 for the 1623 cm^{-1} band indicates that the transverse mode is oriented parallel to the membrane surface and likewise for the longitudinal mode at 1685 cm^{-1}. The tilt angle of the β-sheet is γ ∼70° relative to the membrane normal for both oxidized and unoxidized membranes, indicating that the β-sheet is preferentially oriented parallel to the membrane surface in both cases.

When proteins in the subphase of a Langmuir trough insert into monolayers, they displace lipid molecules laterally and cause the surface pressure to increase. Surface pressure measurements when Aβ42 was injected into the subphase yielded two surprising results. First, Aβ42 did not change the membrane surface pressure (20 dynes/cm) in any of the five membrane preparations. This indicates that Aβ42 does not insert into the membranes far enough to displace lipids laterally. Second, high surface pressure (>35 dynes/cm) dramatically reduced protein adsorption to oxidized membranes and eliminated almost all spectral evidence for the formation of β-structure (discussed below). There is intense dispute over the monolayer pressure that corresponds to the internal pressure of a lipid bilayer, but most estimates place the value between the extremes of 20 and 35 dyn/cm that we have examined.

The various lipid absorptions are present in the background spectra and therefore their absorption bands do not appear in the final collected spectra. However, if the lipid orientation

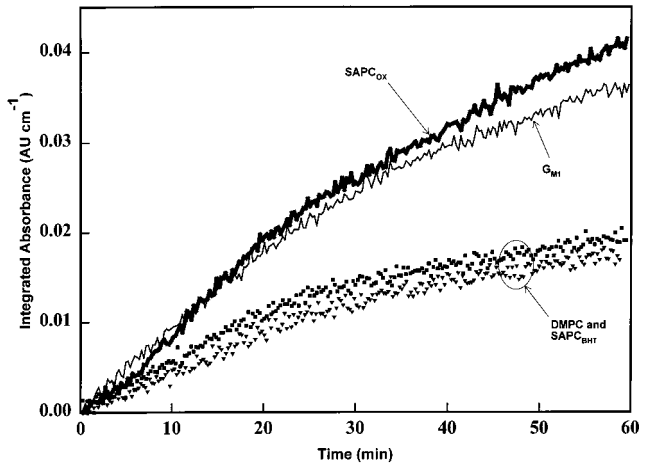

FIGURE 3: Kinetics of Aβ42 adsorption by phospholipid monolayers, measured by the integrated absorbance of the band at ~1624 cm^{-1} versus time. Thick solid line, 20 mol % oxidized SAPC and 80 mol % DMPC; thin solid line, 3 mol % G_{M1} and 97 mol % DMPC; small squares, 100% DMPC; small triangles, 20 mol % unoxidized SAPC and 80 mol % DMPC with 1 mol % BHT. Each curve represents an average of three separate experiments, each performed on different days in random sequence.

was significantly perturbed we would see complementary positive and negative difference bands in the parallel and perpendicularly polarized spectra, and if lipids were displaced from the crystal surface, there would be negative difference bands in both polarized spectra (e.g., ref *45*). Neither of these spectral features are seen, so we conclude that membrane structure is not significantly perturbed by Aβ42 adsorption. This is consistent with our conclusion above that Aβ42 does not penetrate into the membranes and displace lipids laterally. Without lipid signals to calibrate these spectra, we are unable to measure protein:lipid ratios or the surface concentration of the protein. Based on typical signal amplitudes, however, it appears that the mole ratio of Aβ42 to lipid after 60 min of accumulation is approximately 1:100.

Experiments were also performed in the absence of lipid membranes, using only a hydrophobic (silane-treated) crystal on the surface of the Langmuir trough. These experiments yielded valuable information because the protein that accumulates in the absence of a membrane absorbs primarily at 1648 cm^{-1} and has very little signal characteristic of β-sheet. This demonstrates that Aβ42 does not adopt a β-sheet conformation in the subphase, and that it is the presence of a membrane, specifically an oxidatively damaged membrane, that induces Aβ42 to assume an antiparallel β-structure.

Kinetics of Aβ42 Adsorption. Differences in the rate of adsorption of protein to membranes in these experiments are significant because the subphase buffer contains the same concentration of protein in each case (0.3 μM). Infrared spectra were recorded at regular time intervals over a 60 min period to document the adsorption rate and conformation of Aβ42 over time.

Integrated areas for the 1624 cm^{-1} band are presented in Figure 3 for four different membrane preparations: 100% DMPC, unoxidized SAPC/DMPC with BHT ($SAPC_{BHT}$), oxidized SAPC/DMPC ($SAPC_{ox}$), and G_{M1}/DMPC. Each data point represents the average of corresponding time points in 3−5 experiments each conducted on different days. The overall rate at which Aβ42 adsorbs to $SAPC_{ox}$ and G_{M1}/DMPC membranes is approximately 2-fold greater than that seen with $SAPC_{BHT}$ and DMPC membranes. The amide I band shape for Aβ42 bound to membranes consisting of G_{M1}/DMPC was similar to that of $SAPC_{OX}$ shown in Figure 2, panels a and b, while the amide I band shape of Aβ42 bound to unoxidized membranes SAPC/DMPC in the presence of BHT was similar to that of DMPC shown in Figure 2, panels c and d.

Two key control experiments were performed. In the first, BHT was added *after* SAPC oxidation. The rate of Aβ42 accumulation in this case was unaffected, demonstrating that the lower accumulation rate seen with $SAPC_{BHT}$ was not due simply to the presence of BHT. In the second, we attempted to characterize Aβ42 accumulation on unoxidized SAPC/DMPC ($SAPC_{UNOX}$) membranes in the absence of BHT to compare accumulation rates on $SAPC_{OX}$ and $SAPC_{UNOX}$ membranes. However, there was no difference between these preparations. As we anticipated, unsaturated lipids in a monolayer at an air−water interface are highly susceptible to spontaneous air oxidation. Despite our best efforts to enclose the Langmuir trough in an argon-filled chamber, the characteristic H−C═C−H stretching mode of olefinic groups at 3012 cm^{-1} (*52*) have lifetimes of less than 15 min the air−water interface (unpublished data). Thus, we rely on our demonstration that BHT does not slow the accumulation of Aβ42 to establish that oxidative damage—and not the lack of BHT—is the cause of increased Aβ42 accumulation on $SAPC_{OX}$ membranes.

The antioxidants α-tocopherol and ascorbate are less effective at inhibiting lipid peroxidation in lipid monolayers. Although α-tocopherol can be pro-oxidant under some circumstances, the more likely reason for its lower effectiveness is that it is relatively volatile. Therefore, it is likely to evaporate when it partitions to a lipid monolayer at the air−water interface of a Langmuir trough. The most likely reason that ascorbate is less effective is that it is water soluble, and does not partition to the monolayer.

DISCUSSION

Our principal finding is that oxidatively damaged lipids accelerate the accumulation of Aβ42 in a β-sheet conformation on lipid membranes. Several key results and control experiments rule out other possible explanations for the observed effects, and support the significance of this observation.

First, $SAPC_{OX}$ membranes accumulated Aβ42 at the same rate whether or not BHT is present. This demonstrated that BHT slowed Aβ42 accumulation onto $SAPC_{BHT}$ membranes by inhibiting the oxidation of SAPC rather than by merely being present in the membrane. It also demonstrated that accelerated Aβ42 accumulation in $SAPC_{OX}$ membranes was not merely due to the presence of unsaturated lipid. These demonstrations are important because the unsaturated acyl chains of SAPC undergo spontaneous oxidation at the air−water interface, precluding a direct comparison of Aβ42 accumulation on $SAPC_{OX}$ and $SAPC_{UNOX}$ membranes.

Second, we demonstrated that small amounts of G_{M1} ganglioside caused the same acceleration of Aβ42 accumulation as $SAPC_{OX}$ and confirmed the effects of G_{M1} on the binding and conformation of amyloid β-proteins noted earlier by others using different techniques (*15*, *29*−*31*). These are

key results because it has been demonstrated that G_{M1}-containing membranes accelerate fibril formation (*29*).

Third, we observed that Aβ42 accumulation is attenuated by high membrane surface pressure. This is a striking result because Aβ42 does not insert into low-pressure membranes (i.e., Aβ42 does not cause membrane area to increase at low pressure). Therefore, the consequence of high pressure is not to prevent the protein from penetrating into the membrane, but instead it appears to change some property of the membrane that is critical to β-sheet formation. Presumably, Aβ42 accumulation and β-structure formation depends on direct interaction between the protein and a lipid component that becomes inaccessible at high pressure. These lipid components might well be the oxidized olefinic groups or the peptide group of G_{M1} that migrate toward the aqueous phase at low pressures because of their increased hydrophilicity.

Our experiments were prompted by published (*53*) and unpublished observations in our laboratory indicating that many proteins and polypeptides form β-structure as they insert into lipid membranes. We had hypothesized that oxidatively damaged lipid acyl chains would facilitate this process in Aβ42 by furnishing hydrogen bond partners to nascent β-structure. While it is clear that oxidatively damaged lipids do indeed facilitate the formation of β-structure by Aβ42, this protein differs from all others we have studied in that it does not insert into the membrane.

The formation of Aβ-protofibrils from Aβ40 has recently been characterized by atomic force microscopy (AFM) on mica and oxidized graphite (*54*). Protofibrils are believed to be nonfibrillar oligomeric intermediates in the formation of fibrils from monomeric Aβ-proteins, and a variety of arguments support the idea that they may be the pathogenic form of these proteins (*54*). Other AFM studies have demonstrated that Aβ42 can also form linear aggregates on mica resembling the protofibrils of Aβ40, but that Aβ42 forms thinner elongated structures on graphite (*55*). The Aβ42 structures that formed on graphite exhibited periodic features consistent with β-sheets, and they accumulated with a time course similar to that of our spectroscopic signals.

At this point, it is not clear whether oxidatively damaged lipid membranes bear a closer physicochemical resemblance to mica, graphite, or oxidized graphite, but it is clear that our spectroscopic results correlate with three important results from these AFM studies: (a) key intermediates in the formation of amyloid fibrils accumulate on various surfaces with time courses measured in minutes, rather than days; (b) the structure of these intermediates is profoundly sensitive to the nature of the surface material; and (c) at least one of these intermediate forms exhibits features suggesting β-sheet structure.

We have considered whether oxidized and G_{M1}-containing membranes do not actually accelerate the formation of β-structure by Aβ42, but instead merely accelerate the adsorption of Aβ42 with preformed β-structure from the subphase buffer. This seems unlikely because the protein that accumulates in the absence of a membrane has a different conformation. In addition, we guard against aggregation and fibril formation in the subphase buffer by using a protein concentration of only 300 nM, which is below its thermodynamic solubility limit. However, even if oxidized and G_{M1}-containing membranes accelerate the adsorption of β-structure rather than its formation, the finding remains significant because it means that these membranes serve as a nidus for the accumulation of abnormal Aβ-proteins.

It is important to recognize the significant technical differences between the experiments on Aβ42 we have described, and those described in an earlier study of Aβ40 using another form of PATIR−FTIR spectroscopy (*32*). In the earlier study, protein and lipid mixtures in organic solvent were dried onto an internal reflection crystal and overlaid with a piece of wet filter paper to produce partially ordered multibilayers ($S_{LIPID} \sim 0.5$). One has no control over pH and ionic strength in this type of preparation and given the limited number of water molecules likely to be present, most protein molecules are probably sandwiched between two closely apposed bilayers (*45*). Our technique, on the other hand, examined a much more highly ordered lipid monolayer [typical $S_{LIPID} > 0.8$ for this system (*41*)] with a realistic lipid−water interface to which proteins were able to freely diffuse and adsorb from a buffered solution.

Our data do not address the question of whether amyloid β-proteins are mediators or byproducts of pathogenic process that leads to Alzheimer's Disease, but if they are mediators then our results point to a mechanism whereby oxidative changes may contribute to the early pathogenesis of Alzheimer's Disease, and they suggest how antioxidants such as vitamin E may alter the clinical course of this disease (*40*).

REFERENCES

1. Kang, J., Lemaire, H. G., Unterbeck, A., Salbaum, J. M., Masters, C. L., Grzeschik, K. H., Multhaup, G., Beyreuther, K., and Muller-Hill, B. (1987) *Nature 325*, 733−736.
2. Citron, M., Diehl, T. S., Gordon, G., Biere, A. L., Seubert, P., and Selkoe, D. J. (1996) *Proc. Natl. Acad. Sci. U.S.A. 93*, 13170−13175.
3. Klafki, H., Abramowski, D., Swoboda, R., Paganetti, P. A., and Staufenbiel, M. (1996) *J. Biol. Chem. 271*, 28655−28659.
4. Hartmann, T., Bieger, S. C., Bruhl, B., Tienari, P. J., Ida, N., Allsop, D., Roberts, G. W., Masters, C. L., Dotti, C. G., Unsicker, K., and Beyreuther, K. (1997) *Nat. Med. 3*, 1016−1020.
5. Figueiredo-Pereira, M. E., Efthimiopoulos, S., Tezapsidis, N., Buku, A., Ghiso, J., Mehta, P., and Robakis, N. K. (1999) *J. Neurochem. 72*, 1417−1422.
6. Yankner, B. A., Duffy, L. K., and Kirschner, D. A. (1990) *Science 250*, 279−282.
7. Hensley, K., Carney, J. M., Mattson, M. P., Aksenova, M., Harris, M., Wu, J. F., Floyd, R. A., and Butterfield, D. A. (1994) *Proc. Natl. Acad. Sci. U.S.A. 91*, 3270−3274.
8. Behl, C., Davis, J. B., Lesley, R., and Schubert, D. (1994) *Cell 77*, 817−827.
9. Roher, A. E., Chaney, M. O., Kuo, Y. M., Webster, S. D., Stine, W. B., Haverkamp, L. J., Woods, A. S., Cotter, R. J., Tuohy, J. M., Krafft, G. A., Bonnell, B. S., and Emmerling, M. R. (1996) *J. Biol. Chem. 271*, 20631−20635.
10. Lambert, M. P., Barlow, A. K., Chromy, B. A., Edwards, C., Freed, R., Liosatos, M., Morgan, T. E., Rozovsky, I., Trommer, B., Viola, K. L., Wals, P., Zhang, C., Finch, C. E., Krafft, G. A., and Klein, W. L. (1998) *Proc. Natl. Acad. Sci. U.S.A. 95*, 6448−6453.
11. Mori, H., Takio, K., Ogawara, M., and Selkoe, D. J. (1992) *J. Biol. Chem. 267*, 17082−17086.
12. Miller, D. L., Papayannopoulos, I. A., Styles, J., Bobin, S. A., Lin, Y. Y., Biemann, K., and Iqbal, K. (1993) *Arch. Biochem. Biophys. 301*, 41−52.
13. Castano, E. M., Prelli, F., Soto, C., Beavis, R., Matsubara, E., Shoji, M., and Frangione (1996) *J. Biol. Chem. 271*, 32185−32191.

14. Selkoe, D. J. (1995) *Nat. Med. 1*, 998−999.
15. Yanagisawa, K., Odaka, A., Suzuki, N., and Ihara, Y. (1995) *Nat. Med. 1*, 1062−1066.
16. Iwatsubo, T., Saido, T. C., Mann, D. M., Lee, V. M., and Trojanowski, J. Q. (1996) *Am. J. Pathol. 149*, 1823−1830.
17. Cook, D. G., Forman, M. S., Sung, J. C., Leight, S., Kolson, D. L., Iwatsubo, T., Lee, V. M. Y., and Doms, R. W. (1997) *Nat. Med. 3*, 1021−1023.
18. Lichtenthaler, S. F., Wang, R., Grimm, H., Uljon, S. N., Masters, C. L., and Beyreuther, K. (1999) *Proc. Natl. Acad. Sci. U.S.A. 96*, 3053−3058.
19. Jarrett, J. T., and Lansbury, P. T., Jr. (1993) *Cell 73*, 1055−1058.
20. Jarrett, J. T., Berger, E. P., and Lansbury, P. T., Jr. (1993) *Biochemistry 32*, 4693−4697.
21. Harper, J. D., and Lansbury, P. T., Jr. (1997) *Annu. Rev. Biochem. 66*, 385−407.
22. Pitschke, M., Prior, R., Haupt, M., and Riesner, D. (1998) *Nat. Med. 4*, 832−834.
23. Shen, C. L., and Murphy, R. M. (1995) *Biophys. J. 69*, 640−651.
24. Terzi, E., Holzemann, G., and Seelig, J. (1995) *J. Mol. Biol. 252*, 633−642.
25. Wood, S. J., Maleeff, B., Hart, T., and Wetzel, R. (1996) *J. Mol. Biol. 256*, 870−877.
26. Terzi, E., Holzemann, G., and Seelig, J. (1997) *Biochemistry 36*, 14845−14852.
27. Shin, R. W., Ogino, K., Kondo, A., Saido, T. C., Trojanowski, J. Q., Kitamoto, T., and Tateishi, J. (1997) *J. Neurosci. 17*, 8187−8193.
28. McLaurin, J., and Chakrabartty, A. (1997) *Eur. J. Biochem. 245*, 355−363.
29. Choo-Smith, L. P., Garzon-Rodriguez, W., Glabe, C. G., and Surewicz, W. K. (1997) *J. Biol. Chem. 272*, 22987−22990.
30. Choo-Smith, L. P., and Surewicz, W. K. (1997) *FEBS Lett. 402*, 95−98.
31. McLaurin, J., Franklin, T., Fraser, P. E., and Chakrabartty, A. (1998) *J. Biol. Chem. 273*, 4506−4515.
32. Matsuzaki, K., and Horikiri, C. (1999) *Biochemistry 38*, 4137−4142.
33. White, D. A. (1973) *The Phospholipid Composition of Mammalian Tissue*, Elsevier, New York.
34. Witztum, J. L. (1994) *Lancet 344*, 793−795.
35. Smith, M. A., Sayre, L. M., Monnier, V. M., and Perry, G. (1995) *Trends Neurosci. 18*, 172−176.
36. Knight, J. A. (1997) *Ann. Clin. Lab. Sci. 27*, 11−25.
37. Knight, J. A. (1998) *Ann. Clin. Lab. Sci. 28*, 331−346.
38. Jeandel, C., Nicolas, M. B., Dubois, F., Nabet-Belleville, F., Penin, F., and Cuny, G. (1989) *Gerontology 35*, 275−282.
39. Zaman, Z., Roche, S., Fielden, P., Frost, P. G., Niriella, D. C., and Cayley, A. C. (1992) *Age Aging 21*, 91−94.
40. Sano, M., Ernesto, C., Thomas, R. G., Klauber, M. R., Schafer, K., Grundman, M., Woodbury, P., Growdon, J., Cotman, D. W., Pfeiffer, E., Schneider, L. S., and Thal, L. J. (1997) *N. Engl. J. Med. 336*, 1216−1222.
41. Axelsen, P. H., Kaufman, B. K., McElhaney, R. N., and Lewis, R. N. A. H. (1995) *Biophys. J. 69*, 2770−2781.
42. Axelsen, P. H., Braddock, W. D., Brockman, H. L., Jones, C. M., Dluhy, R. A., Kaufman, B. K., and Puga, F. J., II (1995) *Appl. Spectrosc. 49*, 526−531.
43. Citra, M. J., and Axelsen, P. H. (1996) *Biophys. J. 71*, 1796−1805.
44. Axelsen, P. H., and Citra, M. J. (1997) *Prog. Biophys. Mol. Biol. 66*, 227−253.
45. Silvestro, L., and Axelsen, P. H. (1998) *Chem. Phys. Lipids 96*, 69−80.
46. Silvestro, L., and Axelsen, P. H. (1999) *Biochem. 38*, 113−121.
47. Bartlett, G. R. (1959) *J. Biol. Chem. 234*, 466−468.
48. Vossen, R. C. R. M., van Dam-Mieras, M. C. E., Hornstra, G., and Zwaal, R. F. A. (1993) *Lipids 28*, 857−861.
49. Marsh, D. (1997) *Biophys. J. 72*, 2710−2718.
50. Krimm, S., and Bandekar, J. (1986) *Adv. Protein Chem. 38*, 181−364.
51. de Jongh, H. H., Goormaghtigh, E., and Ruysschaert, J. M. (1996) *Anal. Biochem. 242*, 95−103.
52. Sills, R. H., Moore, D. J., and Mendelsohn, R. (1994) *Anal. Biochem. 218*, 118−123.
53. Wimley, W. C., Hristova, K., Ladokhin, A. S., Silvestro, L., Axelsen, P. H., and White, S. H. (1998) *J. Mol. Biol. 277*, 1091−1110.
54. Harper, J. D., Wong, S. S., Lieber, C. M., and Lansbury, P. T. (1999) *Biochemistry 38*, 8972−8980.
55. Kowalewski, T., and Holtzman, D. M. (1999) *Proc. Natl. Acad. Sci. U.S.A. 96*, 3688−3693.

BI000619D